Proceedings of ASME 2022 International Additive Manufacturing Conference
I-AM 2022
October 19-20, 2022, Lisbon, Portugal

IAM2022-96840

DATA-DRIVEN MODEL PREDICTIVE CONTROL FOR ROLL-TO-ROLL PROCESS REGISTER ERROR

Karan Shah
Mechanical and Industrial Engineering
Northeastern University
Boston, Massachusetts 02115
Email: shah.karan@northeastern.edu

Anqi He
Mechanical and Industrial Engineering
Northeastern University
Boston, Massachusetts 02115
Email: he.an@northeastern.edu

Zifeng Wang
Mechanical and Industrial Engineering
Northeastern University
Boston, Massachusetts 02115
Email: wang.zifen@northeastern.edu

Xian Du
Mechanical and Industrial Engineering
University of Massachusetts Amherst
Amherst, Massachusetts 01003
Email: xiandu@umass.edu

Xiaoning Jin*
Mechanical and Industrial Engineering
Northeastern University
Boston, Massachusetts 02115
Email: xi.jin@northeastern.edu

ABSTRACT

Roll-to-Roll (R2R) printing techniques are promising for high-volume continuous production of substrate-based products, as opposed to sheet-to-sheet (S2S) approach suited for low-volume work. However, meeting the tight alignment tolerance requirements of additive multi-layer printed electronics specified by device resolution that is usually at micrometer scale has become a major challenge in R2R flexible electronics printing, preventing the fabrication technology from being transferred from conventional S2S to high-speed R2R production. Print registration in a R2R process is to align successive print patterns on the flexible substrate and to ensure quality printed devices through effective control of various process variables. Conventional model-based control methods require an accurate web-handling dynamic model and real-time tension measurements to ensure control laws can be faithfully derived. For complex multi-stage R2R systems, physics-based state-space models are difficult to derive, and real-time tension measurements are not always acquirable. In this paper, we present a novel data-driven model predictive control (DD-MPC) method to minimize the multistage register errors effectively. We show that the DD-MPC can handle multi-input and multi-output systems and obtain the plant model from sensor data via an Eigensystem Realization Algorithm (ERA) and Observer Kalman filter identification (OKID) system identification method. In addition, the proposed control scheme works for systems with partially measurable system states.

Keywords: Roll-to-roll, Data-driven, Model Predictive Control, Register Control

INTRODUCTION

Fabrication of substrate-based products traditionally adopts a sheet-to-sheet (S2S) approach for multi-layer printing due to its higher printing accuracy. However, S2S is a slow process that is more appropriate for low-volume production. A high-volume continuous production process, such as Roll-to-Roll (R2R) printing process, is highly desirable provided the tight alignment tolerance requirements of additive multi-layer printed electronics are met. These tolerances are device resolution specified that generally require micrometer accuracy. This is a major hurdle for R2R flexible electronics printing, preventing the fabrication industry to shift to the high-speed R2R approach from conven-

*Address all correspondence to this author.

tional S2S approach. Registration of multiple layers on a flying substrate is important. Print registration in a printing process is to align successively print patterns on the material and to ensure a quality print output through appropriately controlling various web handling process variables, such as web transport velocity, web tension, web strain, etc [1]. Register errors refer to the position misalignment between the two adjacent overlapped patterns [2]. Surface integrity of printed layers and poor registration accuracy of the source-drain electrodes to the gate electrode generate severe problems such as missing or disconnected printing patterns, and thus printed devices malfunction that seriously impedes the successful deployment of full-scale processes for R2R electronics printing.

Related Work

R2R system is a complex system that involves multiple operational parameters that exhibit a nonlinear system behavior. This nonlinear input-output behavior is mainly caused by two sources of variability: substrate related and roller related variability. Problems such as lay flats, curls, wrinkling, slip conditions, are caused by variations and uncertainty in substrate materials and their condition in process. Roller roundness error, roller wear and tear, imbalance are also commonly seen issues causing nonlinear dynamics and misalignment. While modeling an R2R system, some of these factors can be assumed negligible or non-contributing to the system dynamics under certain operational conditions, however, these factors could significantly affect the system responses such as printed pattern position and dimension. Hence, an accurate model of an R2R system that identifies system input-output relationship is needed for accurate register error estimation, which serves as a prerequisite for effective register control. Typically, a physics-based approach for system modeling is applied to estimate the R2R plant dynamics. A mathematical model about register control of a gravure printing process is proposed in [3] by using the continuum equation and register error equation. However, in several cases, such first-principle based mathematical model for register error estimation is not accessible due to highly nonlinear input-output relationship, disturbances such as slippage, tension fluctuation, and material property variation.

Recent contributions in R2R process control mostly focus on model-based control which refers to plant modeling based on physical laws of the process. Mathematical models representing the real physical dynamics of elements in the system. Different control algorithms based on first-principle based plant models can be designed, i.e., robust H-infinity (H_∞) control, feed forward proportional-derivative (PD) control, proportional-integral-derivative (PID) control, open loop control. Most of these methods require load cell for tension measurements and they are proposed to mainly account for tension and torque control rather than register error control. Data-driven control methods have not been fully investigated and widely adoptive. Artificial neural networks (ANNs) are used to learn the dynamics of plants [4]. Modified genetic algorithms are used to determine the optimal gain of a feedback register controller [5].

Researchers have presented various approaches for achieving high-precision registration in R2R printing. Many works utilizing phase-shifting of the printing cylinder for register control can reduce register error. Most of them use dynamic mathematical models to describe the relationship between phase-shifting of the printing cylinder and tension or register error ([6–8]). Based on these physics-based register models, many researchers have proposed numerous control methods to reduce machine direction (MD) register error. Kang et al. [9] proposed a compensation method based on a PID controller to reduce the register errors for a multistage R2R printing process and this method can also cancel out the upstream disturbance by phase shifting the printing cylinder. Yoshida et al. [10] developed a nonlinear register control method based on a Lyapunov function. Komatsu et al. [11] proposed a delay-dependent nonlinear control approach by adjusting the new coordinate and delay-dependent feedback law. Kang et al. [12] developed a linear quadratic (LQ) regulator to control both the tension and register of a hybrid R2R printing system. The aforementioned control methods all utilize phase-shifting of the printing cylinder to maintain a constant tension in the web or to keep the register error within the acceptable range, but there are still limitations that make it difficult to reduce the register error to smaller scale for high-precision tight-tolerance printing processes, i.e, less than 20 microns. There remain three major barriers to use the existing methods for multistage R2R printing to control overlay register errors at the micrometer scale.

- The register errors in the upstream and downstream can not be completely compensated since only the coupling of the adjacent printing units is considered. As the number of printing cylinders increases, the coupling complexity of these method increases. Therefore, a control method that can consider the coupling of the upstream and downstream registers is needed.
- These model-based control methods require tension measurements since these control rules are derived based on mathematical models. However, not all tension measurements in the desired positions can be provided in practice constrained by cost and installation difficulties.
- These control methods are mainly served for tension control therefore they could be ineffective in register error control, where tension and web speed need to be handled as model constraints.

Recent advances in model predictive control (MPC) have shown that it is an appealing alternative to traditional control schemes as it can learn the optimal control action from data, and handle nonlinear system dynamics by solving an optimization

problem over predicted future outputs of a system. In this paper, we design our control methods based on an MPC scheme for the R2R register control because of the following:

1. MPC can naturally handle multi-input and multi-output systems, which may have couplings between inputs and outputs.
2. MPC can handle situations when some system states (such as tension) cannot be measured.
3. MPC can naturally consider other constraints such as tension, input changing rate since it is built up based on optimization process with different constraints.

For modeling R2R systems, most studies in the literature use physics-based modeling techniques, however data-driven system identification techniques have not been explored as much. Two of the most popular system identification methods are Eigensystem Realization Algorithm (ERA) as proposed by Juang and Pappa [13] and Observer Kalman filter identification (OKID) as proposed by Juang et al. [14]. Due to its high efficiency and versatile algorithm, both ERA and OKID have been prominently used in the aerospace industry where model accuracy is extremely important. ERA has been utilized to study the behavior of aerospace structures by Pappa et al. [15], to design a reduced order model for Tiltrotor aircraft stability analysis by Bath et al. [16], and to identify shape estimation of the flexible spacecraft membranes by Brownell et al. [17]. Similarly, OKID has been utilized for system identification of small unmanned air system by Leshikar, and Valasek [18], and to identify open loop airframe characteristics of an Octocoptor by Iyer et al. [19].

Objectives and Contributions

In this paper, we propose a novel data-driven model predictive control (DD-MPC) scheme for multi-stage register error control in R2R processes. The main advantage of the proposed DD-MPC method over existing feedback and model-based register control methods is that it only requires input-output data but no physics-based model for the online estimation process. Since it uses a data-driven system identification method, the presented scheme relies on output-feedback for MPC design and does not require online state measurements, i.e., web tension, web speed.

System Identification techniques, specifically ERA and OKID, have been proposed to identify R2R system plant using only the input-output data. The main advantage of the proposed techniques is that it does not require prior knowledge of the R2R system or the underlying physics that govern it. For the ERA method, system response to an impulse input and for the OKID method, system response to a pseudo random input is sufficient to derive the R2R system dynamics. For the proposed identified R2R system, the input parameter used is the roller speed, V, while the output parameter used is the register error, Rx.

Structure of the paper

The remainder of this paper is organized as follows. Section 2 provides the preliminaries of physics-based modeling for a multi-stage R2R system and the simulation results to show its efficacy. Section 3 presents the detailed data-driven modeling methods (ERA and OKID) for system identification with model verification and validation. In Section 4, the proposed data-driven system model is integrated into a DD-MPC control scheme design and the performance of register control is evaluated. Section 5 concludes the paper and presents the future works.

PHYSICS-BASED MODEL FOR R2R SYSTEMS

Mathematical Modeling of Register in printing system

We first present the preliminaries of the R2R system modeling – a mathematical model for modeling the dynamics of a three-layer R2R electronics printing system [9]. The R2R system studied in this paper consists of two adjacent printing rollers, and each printing roller has an impression roller on the top, a gravure cylinder, and a register error scanning sensor, shown in Fig. 1. We assume that all printing cylinders are controlled to preserve the same phase. The tension of the substrate entering the first printing cylinder (T_1) is controlled for maintaining constant tension, and the first printing cylinder rotates at a constant velocity as a master speed drive. The first printing roller prints the pattern of a white square on the web. The web is then moved to the second printing roller and a gray pattern is printed by the second printing roller. Finally, a black square is printed by the third printing roller. The register error Rx_i (i = 2, 3) is defined as the relative distance difference between two printed patterns, which are printed by the adjacent printing rollers. The variable ε_i (i = 2, 3) denotes the strain of a substrate between the $(i-1)^{th}$ and i^{th} printing rollers. Particularly, ε_1 denotes the strain at the inlet of the first printing unit, which is associated with a tension control system to maintain the web tension at a constant level. The corresponding tension T_i (i = 1, 2, 3) is determined by the formula $T = AE\varepsilon$, where A is cross sectional area of the web and E is Young's modulus; L_u and L_d are the web length between corresponding printing rollers; v_i is the tangential velocity of i^{th} printing cylinder.

Since the register error is affected by the strain of the moving web and the variation of velocity of the printing cylinder [9], the relationship between the register errors and variation of the tangential velocity of i^{th} printing cylinder in the R2R system can be linearized by perturbation method and expressed as the following equations from [9]:

$$
\begin{aligned}
\Delta\dot{T}_2(t) &= \frac{1}{L_u}(v_{10}\Delta T_1(t) - v_{20}\Delta T_2(t)) \\
&\quad + \frac{AE}{L_u}(\Delta V_2(t) - \Delta V_1(t)) \\
\dot{R}x_2(t) &= \frac{1}{AE}(v_{10}\Delta T_1(t-\tau_u) - v_{20}\Delta T_2(t)) \\
\Delta\dot{T}_3(t) &= \frac{1}{L_d}(v_{20}\Delta T_2(t) - v_{30}\Delta T_3(t)) \\
&\quad + \frac{AE}{L_u}(\Delta V_3(t) - \Delta V_2(t)) \\
\dot{R}x_3(t) &= \frac{1}{AE}(v_{10}\Delta T_2(t-\tau_d) - v_{30}\Delta T_3(t))
\end{aligned} \tag{1}
$$

where $\Delta T_i(t)$ is the variation of the tension and $\Delta V_i(t)$ is the variation of the gravure cylinder's tangential velocity; v_{i0} represents the operating speed of the web at the steady state.

For a multi-layer R2R process as presented, there are multiple printing rollers that print different layers to collectively print the required pattern. The transportation time for a single point on a substrate to travel from one printing head to another is essentially the time lag or the time delay term τ in equation (1). This means that τ accounts for the delay between the printing of each layer in the process. For any two printing rollers in sequence, τ can be calculated using the formula $\tau = L/v$, where L is the span length or the distance between the two rollers and v is the operating velocity of the web.

The linear, continuous space-state model of the R2R system can be further expressed in the general form as follows:

$$
\begin{aligned}
\dot{X}(t) &= AX(t) + A'X(t-\tau_d) + BU(t) \\
Y(t) &= CX(t)
\end{aligned} \tag{2}
$$

where $X(t) = \begin{bmatrix} Rx_2(t) \\ Rx_3(t) \\ \Delta T_2(t) \\ \Delta T_2(t) \end{bmatrix}$, $U(t) = \begin{bmatrix} \Delta V_2(t) \\ \Delta V_3(t) \end{bmatrix}$, $A = \begin{bmatrix} 0 & 0 & -\frac{v}{AE} & 0 \\ 0 & 0 & 0 & -\frac{v}{AE} \\ 0 & 0 & -\frac{v}{L_u} & 0 \\ 0 & 0 & \frac{v}{L_d} & -\frac{v}{L_d} \end{bmatrix}$, $A' = \begin{bmatrix} 0 & 0 & 0 & 0 \\ 0 & 0 & \frac{v}{AE} & 0 \\ 0 & 0 & 0 & 0 \\ 0 & 0 & 0 & 0 \end{bmatrix}$, $B = \begin{bmatrix} 0 & 0 \\ 0 & 0 \\ \frac{AE}{L_u} & 0 \\ -\frac{AE}{L_d} & \frac{AE}{L_d} \end{bmatrix}$, $C = \begin{bmatrix} 1 & 0 & 0 & 0 \\ 0 & 1 & 0 & 0 \\ 0 & 0 & 0 & 0 \\ 0 & 0 & 0 & 0 \end{bmatrix}$.

Simulation Result and Parameter Sensitivity Analysis

The numerical simulations were performed to validate Model of Register in printing system in various operating conditions. The simulation conditions were summarized in Table 1.

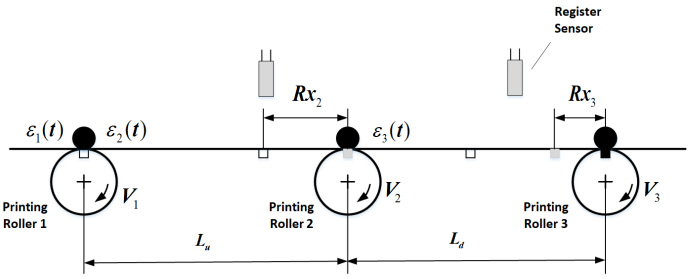

FIGURE 1: THE ILLUSTRATION OF A THREE-LAYER ROLL-TO-ROLL PRINTING SYSTEM

The pulse velocity of V_2 is generated in the second printing roller as an input at time 10 s. The pulse responses of register and tension were illustrated in Fig. 2(a) and Fig. 2(b), respectively. The input of V_2 was conducted as 0.001 m/s during 1 s, therefore the phase of the second printing roller varies in 1 mm. At steady state, the absolute magnitude of the register is the same as the phase variation of 1 mm in the upstream and downstream directions, denoted as e_2 and e_3, respectively, as shown in Fig. 2(a). The different signs of the register in the upstream and downstream directions indicate that the second printing pattern was moved in the downstream direction such that the phase between the first cylinder and the second cylinder decreased; otherwise, the phase between the second and the third printing cylinder increased. The pulse input of V_2 generated the transient tension disturbance T_2 between the second and the third printing roll, and in steady state it converges to the initial tension due to the effect of 'tension transfer' as shown in Fig. 2(b). Also, the response times of register and tension were reversely proportional to the operating velocity as shown in Fig. 2(a) and Fig. 2(b).

The step input of T_1 is generated as an input at time 10 s. The step responses of register and tension were illustrated in Fig. 3(a) and Fig. 3(b), respectively. The input tension of T_1 transferred to the downstream, and web tension T_2 and T_3 converged to T_1 by the 'tension transfer' as shown in Fig. 3(b). The step input of T_1 only generated the transient register variation of Rx_2 and Rx_3 as shown in Fig. 3(a). Also, the response times of register and tension were reversely proportional to the operating velocity as shown in Fig. 3(a) and Fig. 3(b).

DATA-DRIVEN MODELING FOR R2R SYSTEMS

In this section, we address the shortcomings of modeling R2R system via a physics-based model by developing a data-driven system identified model. This approach explicitly relies on the available measure data (roller velocity and register error) and doesn't require any prior knowledge of the underlying physical nature of the R2R system. Particularly, we use ERA and

TABLE 1: SIMULATION CONDITIONS

Conditions	Values (units)
Operating Tension	86.5 (N)
Operating Velocity	0.5, 1 (m/s)
Thickness of Substrate	1.2×10^{-5} (m)
Width of Substrate	1 (m)
L_u	4 (m)
L_d	4 (m)
Young's modulus	3.6 (GPa)
Simulation Time	100 (sec)

OKID methods to process the input-output data and extract the system dynamics through a state space model.

Though ERA by itself is an efficient method to derive R2R system dynamics from its input-output data, it specifically requires impulse response data which can be difficult to measure due to physical limitations in the R2R setup. Hence, OKID method is being used as an extension to ERA where the impulse input data is substituted by a pseudo random input data. Both ERA and OKID algorithms for R2R system can efficiently estimate system dynamics and can further be used as a plant for a controller to reduce the register error.

In order to understand these methods, we begin by considering a linear, discrete time, time-invariant dynamical system model using the following state variable equations:

$$\begin{aligned} X_{k+1} &= AX_k + BU_k \\ Y_k &= CX_k + DU_k \end{aligned} \tag{3}$$

Here, X is the n-dimensional state vector, Y is the p-dimensional output vector, U is the m-dimensional input vector, and k is the time sample. A, B, C, and D are constant state matrices.

The following subsections walk through the underlying algorithm for the ERA and OKID methods. Both methods formulate the problem of system realization where given the output measurements, Y_k, to a known input, U_k, the A, B, C, and D matrices are constructed.

Eigensystem Realization Algorithm (ERA)

The ERA method estimates the state matrices using the *Observability* ($\mathscr{O}$) and *Controllability* ($\mathscr{C}$) matrices, when subjected

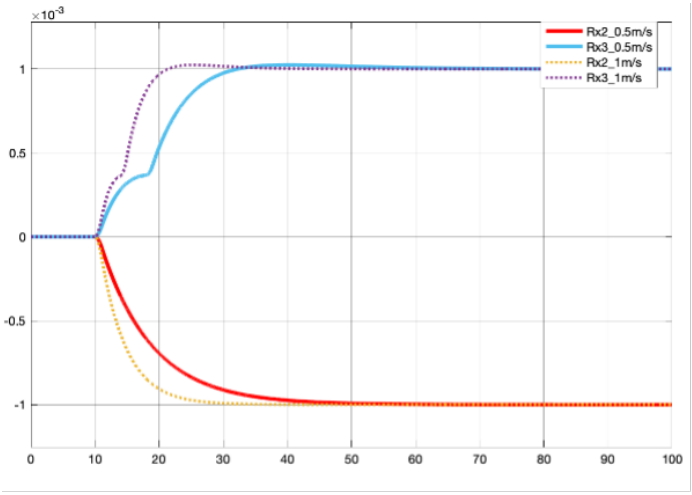

(a) REGISTER ERROR

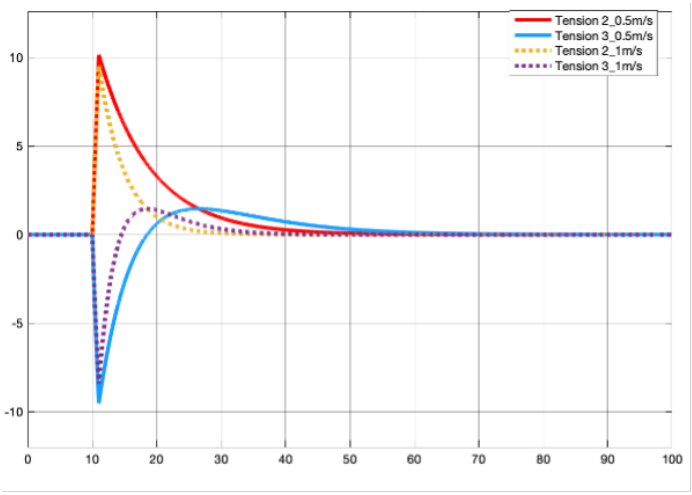

(b) TENSION VARIATION

FIGURE 2: REGISTER ERROR AND TENSION VARIATION CAUSED BY A 0.001 M/S PULSE INPUT APPLIED TO V_2 AT 10 SECS

to a impulse input directly from the output response [13]. ERA does not require prior knowledge of the system, but is entirely based on the impulse response of the system. The corresponding time domain output response Y_k^δ is known as the Markov parameters:

$$Y_k^\delta = \begin{cases} D & \text{k} = 0, \\ CA^{k-1}B & \text{k} > 0 \end{cases} \tag{4}$$

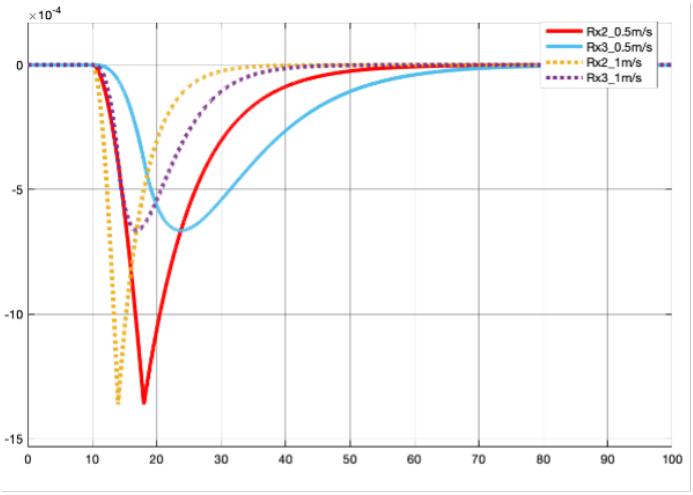

(a) REGISTER ERROR

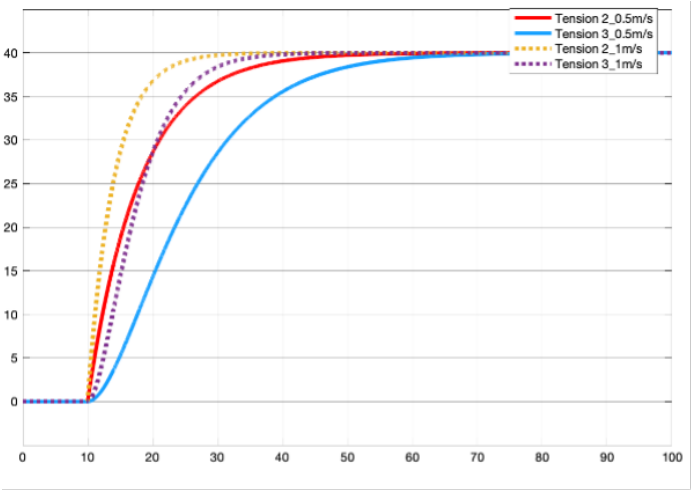

(b) TENSION VARIATION

FIGURE 3: REGISTER ERROR AND TENSION VARIATION CAUSED BY A 40 N STEP INPUT APPLIED TO T_1 AT 10 SECS

When the prior knowledge of system is known, a Hankel matrix, H can be formed as such:

$$H = \mathscr{O}\mathscr{C} \tag{5}$$

where $\mathscr{O}$ is the *Observability* matrix given by:

$$\mathscr{O} = \begin{bmatrix} C \\ CA \\ \vdots \\ CA^{m_o-1} \end{bmatrix}$$

and $\mathscr{C}$ is the *Controllability* matrix given by:

$$\mathscr{C} = \begin{bmatrix} B\ AB \cdots CA^{m_c-1}B \end{bmatrix}$$

Here, m_o and m_c are respective time steps.

Therefore, Hankel matrix is given by:

$$H = \begin{bmatrix} CB & CAB & \cdots & CA^{m_c-1}B \\ CAB & CA^2B & \cdots & CA^{m_c}B \\ \vdots & \vdots & \ddots & \vdots \\ CA^{m_o-1}B & CA^{m_o}B & \cdots & CA^{m_c+m_o-2}B \end{bmatrix} \tag{6}$$

For the current case, the state dynamics, matrices A, B, C, and D, are unknown. Therefore, the same Hankel matrix can be constructed using just the Markov Parameters, resulting in a purely data driven approach for system realization as described below.

Using the Markov parameters, a Hankel matrix as given by (6) can be constructed as such:

$$H = \begin{bmatrix} Y^\delta_1 & Y^\delta_2 & \cdots & Y^\delta_{m_c} \\ Y^\delta_2 & Y^\delta_3 & \cdots & Y^\delta_{m_c+1} \\ \vdots & \vdots & \ddots & \vdots \\ Y^\delta_{m_o} & Y^\delta_{m_o+1} & \cdots & Y^\delta_{m_c+m_o-1} \end{bmatrix} \tag{7}$$

If the definition of Markov parameters from (4) is substituted in (7), then the same Hankel matrix as given by (6) can be extracted.

Also, a shifted Hankel Matrix, H' can be constructed by shifting Markov parameters by one time step unit as given by:

$$H' = \begin{bmatrix} Y^\delta_2 & Y^\delta_3 & \cdots & Y^\delta_{m_c+1} \\ Y^\delta_3 & Y^\delta_4 & \cdots & Y^\delta_{m_c+2} \\ \vdots & \vdots & \ddots & \vdots \\ Y^\delta_{m_o+1} & Y^\delta_{m_o+2} & \cdots & Y^\delta_{m_c+m_o} \end{bmatrix} \tag{8}$$

$$H' = \begin{bmatrix} CAB & CA^2B & \cdots & CA^{m_c}B \\ CA^2B & CA^3B & \cdots & CA^{m_c+1}B \\ \vdots & \vdots & \ddots & \vdots \\ CA^{m_o}B & CA^{m_o+1}B & \cdots & CA^{m_c+m_o-1}B \end{bmatrix} = \mathscr{O}AC \tag{9}$$

Building Singular Value Decomposition (SVD) of H and H', the

following state matrices are extracted:

$$\begin{aligned}\tilde{A} &= \tilde{\Sigma}^{-1/2}\tilde{U}^T H' \tilde{V}\tilde{\Sigma}^{-1/2} \\ \tilde{B} &= \tilde{\Sigma}^{-1/2}\tilde{V}^T \begin{bmatrix} I_p & 0 \\ 0 & 0 \end{bmatrix} \\ \tilde{C} &= \begin{bmatrix} I_q & 0 \\ 0 & 0 \end{bmatrix} \tilde{U}\tilde{\Sigma}^{1/2}\end{aligned} \tag{10}$$

Hence, the discovered model is of the form:

$$\begin{aligned}\tilde{X}_{k+1} &= \tilde{A}\tilde{X}_k + \tilde{B}U_k \\ Y_k &= \tilde{C}\tilde{X}_k + DU_k\end{aligned} \tag{11}$$

where $\tilde{X}$ is the estimated states with estimated $\tilde{A}$, $\tilde{B}$, and $\tilde{C}$ state matrices.

Observer Kalman filter Identification (OKID)

In practical applications, it is difficult to perform an isolated experiment to measure the system response to an impulse input. Moreover, the measurement noise can further make it challenging to measure true system response. Therefore, OKID estimates the impulse response of a system from a pseudo-random input, which can further be passed onto the ERA algorithm [14].

The OKID algorithm uses discrete-time state space model such as (3) but with an optimal observer:

$$\begin{aligned}\hat{X}_{k+1} &= A\hat{X}_k + BU_k + K_o(Y_k - \hat{Y}_k) \\ \hat{Y}_k &= C\hat{X}_k + DU_k\end{aligned} \tag{12}$$

which is equivalent to:

$$\hat{X}_{k+1} = \underbrace{(A - K_o C)}_{\bar{A}}\hat{X}_k + \underbrace{\begin{bmatrix} B - KD & K_o \end{bmatrix}}_{\bar{B}} \begin{bmatrix} U_k \\ Y_k \end{bmatrix} \tag{13}$$

where K_o is the observer gain using which the poles of $\bar{A}$ can be placed anywhere, provided the system is observable.

Next, the following algorithm given by Juang et. al [14], solves for the Observer Markov parameters $\bar{Y}^\delta$ as a function of control input U and measurements Y:

1. Construct the measurement matrix:

$$Y = \begin{bmatrix} y_0 & y_1 & \cdots & y_l & \cdots & y_m \end{bmatrix} \tag{14}$$

   where an appropriate number of observer Markov parameters is chosen to identify l.
2. Construct the control input matrix:

$$U = \begin{bmatrix} u_0 & u_1 & \cdots & u_l & \cdots & u_m \\ 0 & v_0 & \cdots & v_{l-1} & \cdots & v_{m-1} \\ \vdots & \vdots & \ddots & \vdots & \ddots & \vdots \\ 0 & 0 & \cdots & v_0 & \cdots & v_{m-l} \end{bmatrix} \tag{15}$$

   where $v_i = \begin{bmatrix} u_i^T & y_i^T \end{bmatrix}^T$
3. Solve for $\bar{Y}^\delta$ using the equation $Y = \bar{Y}^\delta U$. This can be done by calculating the right pseudo-inverse of U using SVD.

Next, the system Markov parameters, Y_k^δ, can be extracted from the observer Markov parameters, $\bar{Y}_k^\delta$ by ordering it as such:

$$\bar{Y}_k^\delta = \begin{cases} D & \text{k = 0,} \\ \begin{bmatrix} (\bar{Y}^\delta)_k^{(1)} & (\bar{Y}^\delta)_k^{(2)} \end{bmatrix} & \text{k > 0} \end{cases} \tag{16}$$

where $(\bar{Y}^\delta)_k^{(1)} \in \mathbb{R}^{q\times p}$, $(\bar{Y}^\delta)_k^{(2)} \in \mathbb{R}^{q\times q}$, and $y_0^\delta = \bar{Y}_0^\delta = D$

Hence, the system Markov parameters can be constructed for $k > 0$ as such:

$$Y_k^\delta = (\bar{Y}^\delta)_k^{(1)} + \sum_{i=1}^{k} (\bar{Y}^\delta)_i^{(2)} Y_{k-i}^\delta \tag{17}$$

These system Markov parameters can be passed on through ERA algorithm and the system dynamics can be extracted as mentioned in the ERA section.

Note that for either of the data driven methods (ERA or OKID), time lag term τ need not be explicitly calculated as the system is entirely dependent on the measured data. Therefore, the time lag term is by default incorporated in the data.

Model Verification and Validation

The derived system identified model for R2R system using ERA and ERA+OKID methods can be validated by comparing the system response to the physics based-model. Parameter sensitivity analysis for register error as mentioned in Physics-based modeling section is performed to directly compare the results. Fig. 4 summarized the results for the original physics-based system (sub-scripted as *"sys"*), ERA system, and ERA+OKID system. The results can be cross-verified with Fig. 2(a). Same simulation conditions as presented in Table (1) are used for this analysis.

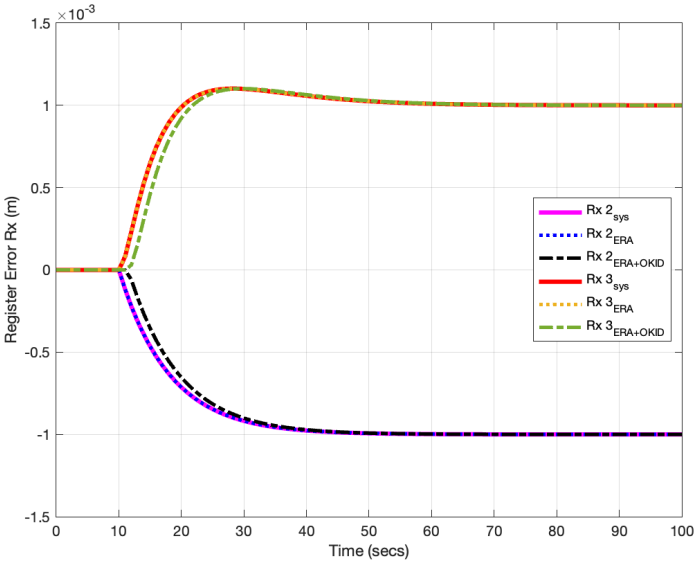

(a) REGISTER ERROR

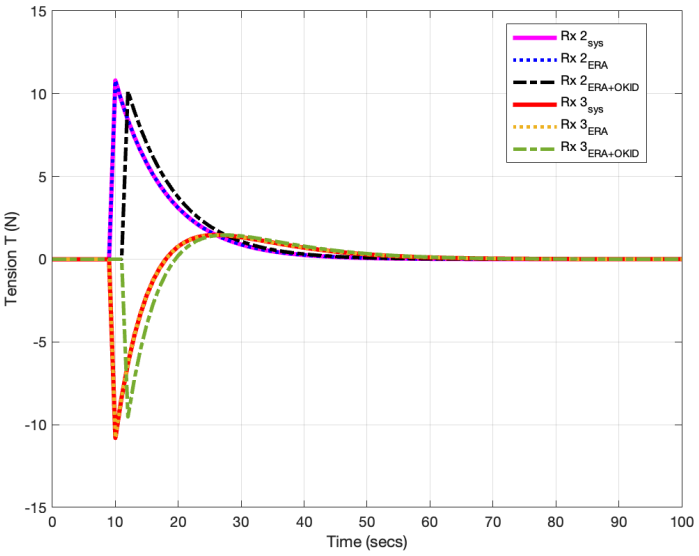

(b) TENSION VARIATION

FIGURE 4: REGISTER ERROR AND TENSION VARIATION CAUSED BY 0.001 M/S PULSE INPUT APPLIED TO V_2 AT 10 SECS FOR DATA DRIVEN METHODS

It can be observed from Fig. 4 that the system response of the identified system using ERA algorithm is nearly identical to the physics-based system's response. Register error for both systems converge with a settling time of approximately 40 seconds and tension variation for both systems converge with a settling time of approximately 50 secs, considering the 2% margin. The system response of the identified system using ERA+OKID algorithm shows a delayed response due zero-initial condition

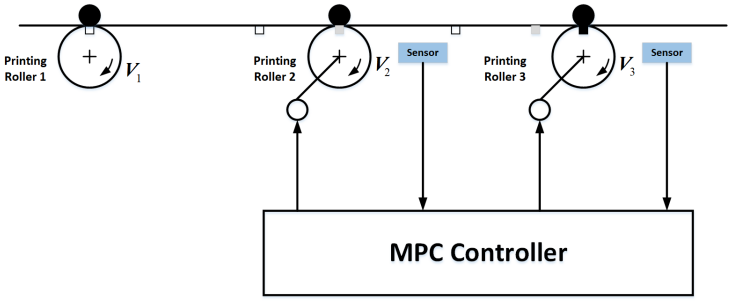

FIGURE 5: MPC SCHEME FOR ROLL-TO-ROLL PRINTING SYSTEMS

Markov parameter ordering ($y_0^\delta = \bar{Y}_0^\delta = D$) in the OKID algorithm (16). Eventually, the system response catches up during the transient response and exhibits a zero steady state error. Note that the steady state error is the error between the physics-based model and the data-driven models.

DATA-DRIVEN MPC (DD-MPC) for REGISTER ERROR CONTROL

In this section, we first developed a physical model-based Model Predictive Control (MPC) for register control in the upstream and downstream simultaneously when all register error measurements can be monitored using error scanning sensors. We compare the model-based MPC with the model-based PID methods to show that the MPC outperforms the others in register error control. This would be used as preliminaries for data-driven MPC approaches, which are based on the proposed ERA and OKID system models developed in the previous section.

Model-based MPC and Performance Analysis

The MPC control scheme is shown as Fig. 5. The error sensors collect the register error measurements from the upstream and downstream printing units of R2R system plant and feed into the MPC controller, which then exports the optimal control inputs into the corresponding printing cylinders in order to stabilize the register error as zero.

For predictive control we need the difference equation model, since we use a discrete time setting. This can be obtained using software such as MATLAB and expressed as the following general form:

$$\begin{aligned} X_{k+1} &= AX_k + BU_k \\ Y_k &= CX_k \\ X_0 &= X(t) \end{aligned} \tag{18}$$

where $X \in \mathbb{R}^n, U \in \mathbb{R}^m, Y \in \mathbb{R}^p, X_k = X(t+k|t), U_k = U(t+k|t)$, k is a nonnegative integer denoting the sample number, which is connected to time by $t = k\Delta$ in which Δ is the sample time.

Given the current state $X(t)$ and $U(t-1)$,we can get the prediction model by iterating the equation (18) as the matrix - vector form:

$$\begin{bmatrix} X_1 \\ \vdots \\ X_{H_u} \\ X_{H_u+1} \\ \vdots \\ X_{H_P} \end{bmatrix} = \underbrace{\begin{bmatrix} A \\ \vdots \\ A^{H_u} \\ A^{H_u+1} \\ \vdots \\ A^{H_P} \end{bmatrix} X_0 + \begin{bmatrix} B \\ \vdots \\ \sum_{i=0}^{H_u-1} A^i B \\ \sum_{i=0}^{H_u} A^i B \\ \vdots \\ \sum_{i=0}^{H_P-1} A^i B \end{bmatrix} U_{-1}}_{\text{past}}$$
$$+ \underbrace{\begin{bmatrix} B & \cdots & 0 \\ AB+B & \cdots & 0 \\ \vdots & \ddots & \vdots \\ \sum_{i=0}^{H_u-1} A^i B & \cdots & B \\ \sum_{i=0}^{H_u-1} A^i B & \cdots & AB+B \\ \vdots & \vdots & \vdots \\ \sum_{i=0}^{H_P-1} A^i B & \cdots & \sum_{i=0}^{H_P-H_u} A^i B \end{bmatrix} \begin{bmatrix} \Delta U_0 \\ \vdots \\ \Delta U_{H_u-1} \end{bmatrix}}_{\text{future}} \tag{19}$$
$$\begin{bmatrix} Y_1 \\ \vdots \\ Y_{H_P} \end{bmatrix} = \begin{bmatrix} C & 0 & \cdots & 0 \\ 0 & C & \cdots & 0 \\ \vdots & \vdots & \ddots & \vdots \\ 0 & 0 & \cdots & C \end{bmatrix} \begin{bmatrix} X_1 \\ \vdots \\ X_{H_P} \end{bmatrix}$$

where $\Delta U_k = \Delta U(t+k|t)$, which is the input increment between time $t+k-1$ and $t+k$:$\Delta U_k = U_k - U_{k-1}$. The prediction horizon has length H_P and the control horizon is H_u . We define the cost function of MPC to be:

$$J(t) = \sum_{k=0}^{H_P} ||Y_k - r_k||^2_{Q(i)} + \sum_{k=0}^{H_u-1} ||\Delta U_k||^2_{R(i)} \tag{20}$$

where r_k is the reference trajectory; $Q(i)$ and $R(i)$ are diagonal weighting matrices. The cost function penalizes deviation of the predicted controlled output from a reference trajectory (In our project the reference trajectory is the vector of zero). The cost function only penalizes changes in the input vector, not its value. We integrate (19) into (20) and the objective of MPC is to solve the following optimization problem known as quadratic programming(QP):

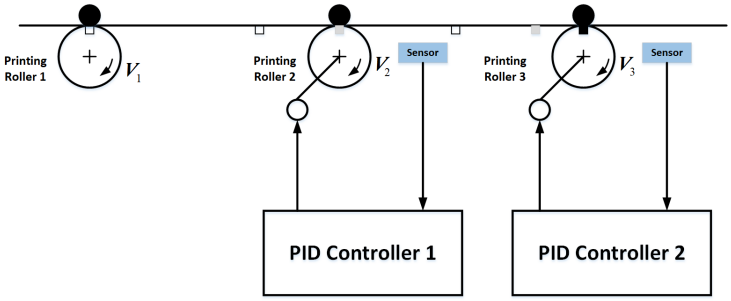

FIGURE 6: DISTRIBUTED PID CONTROL SCHEME FOR ROLL-TO-ROLL PRINTING SYSTEMS

$$\begin{aligned} \min_{\{\Delta U_0, \cdots, \Delta U_{H_u-1}\}} \quad & \sum_{k=0}^{H_P} ||Y_k - r_k||^2_{Q(i)} + \sum_{k=0}^{H_u-1} ||\Delta U_k||^2_{R(i)} \\ s.t. \quad & Y_{min} \le Y_k \le Y_{max}, k = 0, \cdots, H_p \\ & \Delta U_{min} \le U_k \le \Delta U_{max}, k = 0, \cdots, H_u - 1 \end{aligned} \tag{21}$$

We can solve this standard QP problem via dynamic programming or gradient descend method. The control strategy is summarized as follows: At each sampling step t:
1) Measure (or estimate) the current state $X(t)$
2) Get the optimal solution $[\Delta U_0^*, \cdots, \Delta U_{H_u-1}^*]$ thus we can get the optimal input vector $[U_0^*, \cdots, U_{H_u-1}^*]$ of the (20)
3) Apply only $U(t) = U_0^*$, discard the remaining optimal inputs $U_1^*, \cdots, U_{H_u-1}^*$
4) Increase t by 1 and repeat the process from step 1).

In the simulation experiment, we assume that all the states can be measured and there is no measurement noise. We set the initial register error in printing cylinder 2 as $e_2(0) = 1 \times 10^{-3} m$. In the printing cylinder 3, there is no initial register error, $e_3(0) = 0m$. In order to validate the effectiveness of the proposed method, the control performance is compared with a classical distributed PID controller under same simulation conditions, as shown as Fig. 6.

Fig. 7 demonstrates the performance of model-based MPC and PID control methods in the case that a register error of 1 mm is induced to the upstream register e_2 as a disturbance input. Compared to the PID control method, the proposed control method yields considerably better results with regard to the fluctuation in the downstream register error e_3. From Fig. 7(b), we can see that and the proposed method maintains the e_3 within ± 0.2 mm while PID method causes an error fluctuation as up to 0.5 mm. Therefore, this result indicates that the proposed control method is more effective in preventing the upstream register fluctuation being propogated to the downstream register. Also, the control inputs of V_2 and V_3 using PID and the proposed method are compared as shown in Fig. 8 during the control time horizon.

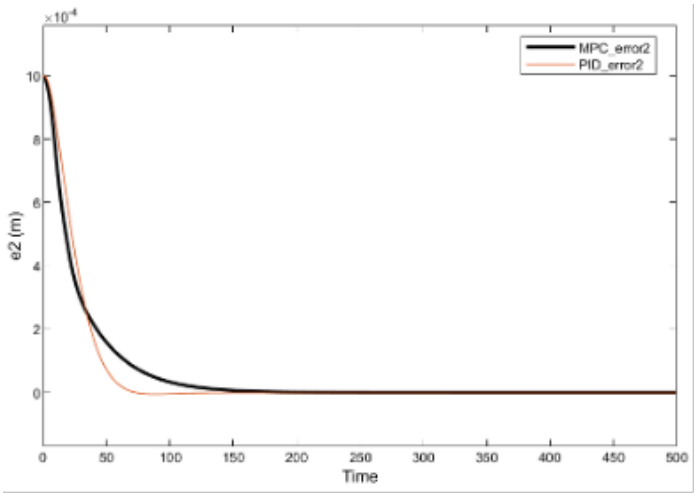

(a) REGISTER ERROR e_2

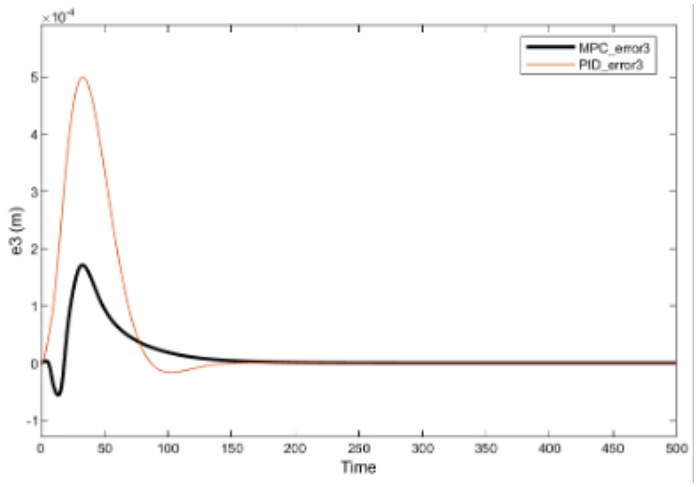

(b) REGISTER ERROR e_3

FIGURE 7: CONTROLLER COMPARISON BETWEEN PID AND MPC CONTROLLERS IN TERMS OF REGISTER ERROR

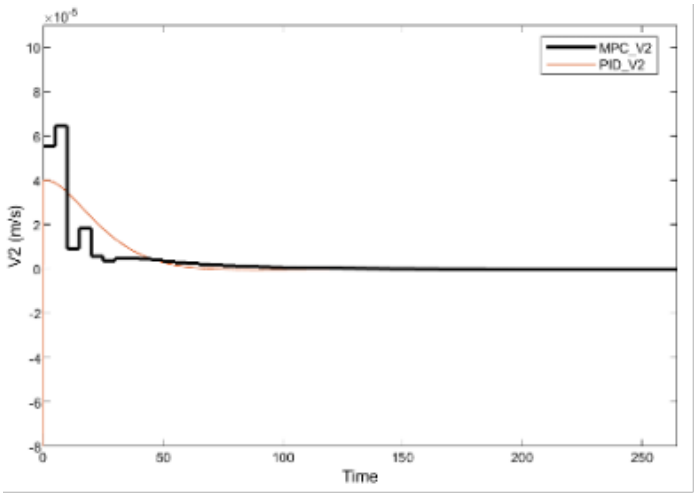

(a) CONTROL INPUT TO ROLLER VELOCITY V_2

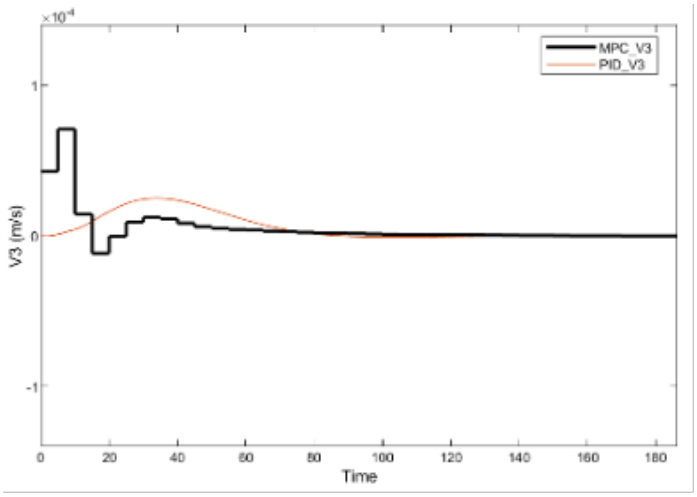

(b) CONTROL INPUT TO ROLLER VELOCITY V_3

FIGURE 8: CONTROLLER COMPARISON BETWEEN PID AND MPC CONTROLLERS IN TERMS OF CONTROL INPUTS

From Fig. 8(a), we observe that PID suffers a large overshoot V_2 at the beginning of the control operation whereas the MPC method can always keep V_2 change smoothly until it reaches steady-state error.

In order to further investigate the robustness of the MPC register control method, we induce white noise to the output of the plant in (2) and we can get:

$$\begin{aligned} X_{k+1} &= AX_k + BU_k \\ Y_k &= CX_k + D_k \\ X_0 &= X(t) \end{aligned} \tag{22}$$

where D_k is the output disturbance. We set the initial register error in printing cylinder 2 as $e_2(0) = 1 \times 10^{-3}$ m. In the printing cylinder 3, there is no initial register error, $e_3(0) = 0$ m. Fig. 8 demonstrates the performance of the MPC and PID control methods in the case of a register error of 1 mm introduced to the upstream register e_2 as a input disturbance. Compared to the PID control method, the proposed control method yields considerably better results with regards to the fluctuation in the downstream register error e_3. From Fig. 7(b), we can see that and the proposed method maintains the e_3 within ± 0.2 mm while the PID method causes an error fluctuation as up to 0.5 mm. In addition, the noise fluctuation level of register error using MPC seems to

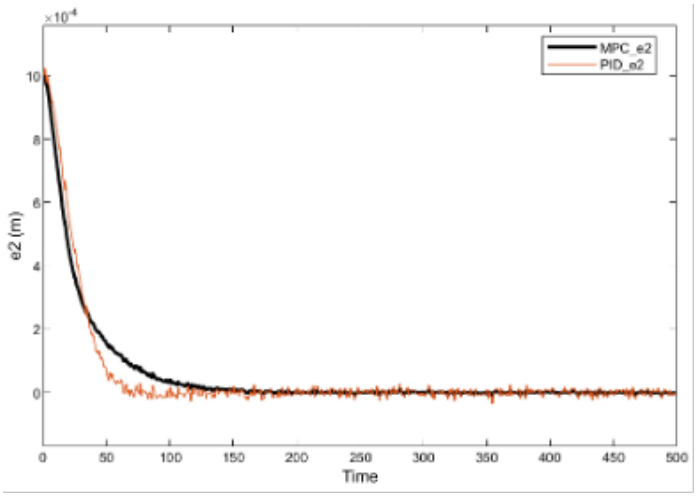

(a) REGISTER ERROR e_2 WITH NOISE

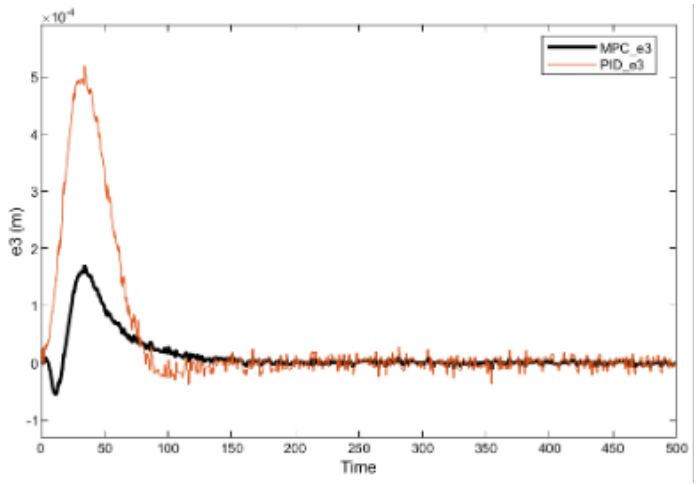

(b) REGISTER ERROR e_3 WITH NOISE

FIGURE 9: OUTPUT RESPONSE FOR VALIDATION OF CONTROL METHOD'S ROBUSTNESS TO NOISE

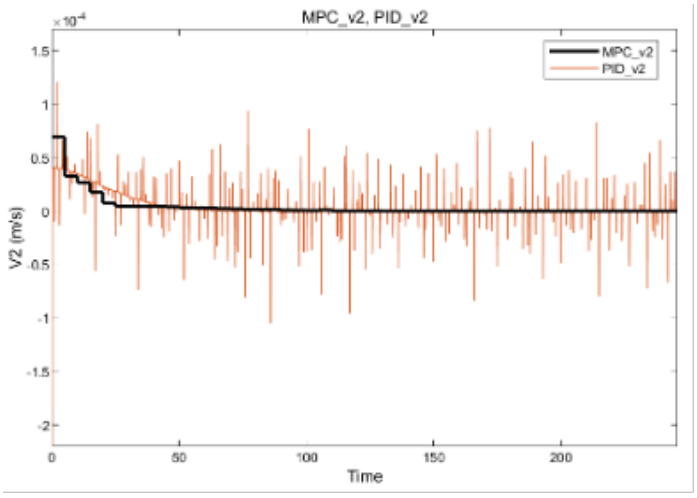

(a) CONTROL INPUT V_2 WITH NOISE

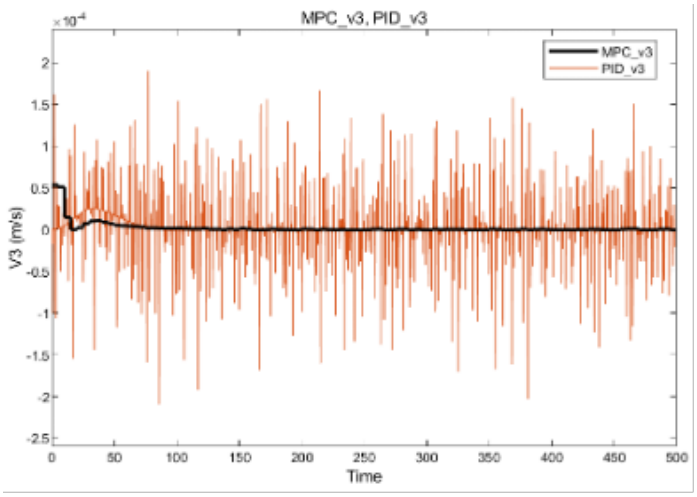

(b) CONTROL INPUT V_3 WITH NOISE

FIGURE 10: CONTROL INPUT FOR VALIDATION OF CONTROL METHOD'S ROBUSTNESS TO NOISE

be lower than PID. Also, the control inputs of ΔV_2 and ΔV_3 using PID and the proposed method are compared as shown in Fig. 9 during the control operation. From Fig. 9(a) and Fig. 9(b), it is obvious that the control input signals of PID show sudden pulses and variation during the entire control process using PID, which may result in the strong impact to the drive motors, deterioration of system stability, and cost of equipment maintenance increasing while the proposed method can always keep ΔV_2 change smoothly because MPC is a constrained optimization method to make overall reduction in variation of the controlled variables.

MPC with ERA and ERA+OKID for Register Control

MPC control scheme as described in the previous section is now extended by applying a MPC controller using system ERA and ERA+OKID models to control register errors. Fig. 11 presents the output response when register error at the second roller is subjected to a initial initial condition of 1 mm. Fig. 12 presents the control inputs as calculated by MPC to achieve the desired results (reference tracking). In ideal condition, the register error is required to be minimal or zero, hence the reference is set to 0. The control horizon is set to 4 and prediction horizon is set to 10 with a sample time of 0.5. For this analysis, controller tuning was done using the MATLAB's MPC designer application to achieve fastest settling time. An aggressive closed-loop

performance and a faster state estimation was chosen to achieve the same. Constraints were only set on the output variables, Rx_2 and Rx_3, to be bounded between $\pm$ 1 mm.

The output response of the DD-MPC can be directly compared to the model-based MPC to evaluate its performance. In the case of model-based MPC control scheme, the plant dynamics are already known based on which an optimal control input is calculated by the MPC controller. This plant is considered as the prediction plant. Then a simulation is run on a simulation plant to check for the MPC performance. Assuming that the physics-based model for R2R is the ground truth model, the prediction plant and the simulation plant will be the same physics-based plant. In the case of DD-MPC control scheme, the plant dynamics are first identified by the data-driven methods. Hence, the prediction plant is set to be the data-driven plants (ERA and ERA+OKID), and the simulation plant is set to be the model-based MPC plant. This is because, in order to validate the performance of our system identified R2R model and the DD-MPC controller, the DD-MPC should be able to effectively control the register error on any kind of R2R system plant, physics-based or data-driven. Therefore, respective plants as mentioned above are used to conduct this performance evaluation analysis.

It can be observed from Fig. 11 that the register error response for both, the MPC with ERA and the MPC with ERA+OKID, reach a steady state in about 30 secs and 40 secs, respectively. When compared with the model-based control methods, as shown in Fig. 7, DD-MPC outperforms both the model-based MPC and the model-based PID in terms of the settling time. This can be due to the non-linear elements in the system model that the physics based may have lacked to capture. Hence, the DD-MPC captures the full dynamics including any non-linear elements that may not be directly modeled.

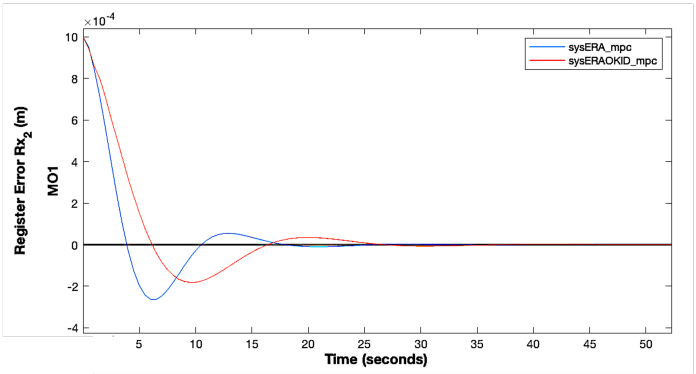

(a) REGISTER ERROR Rx_2

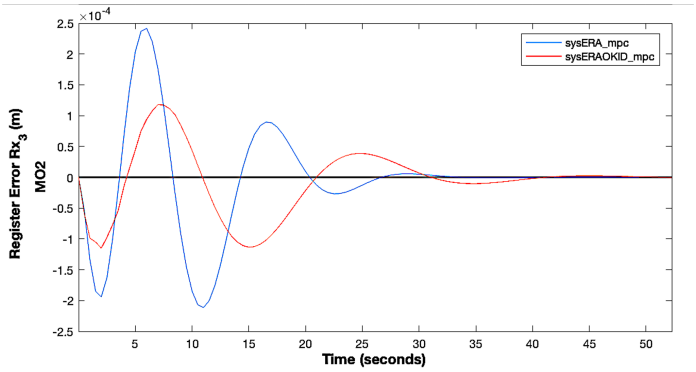

(b) REGISTER ERROR Rx_3

FIGURE 11: REGISTER ERROR RESPONSE TO INITIAL CONDITIONS WITH DD-MPC

CONCLUSION

In this paper, we present a novel data-driven model predictive control method for register control in a multi-stage roll-to-roll printing system. We've shown the efficacy of an ERA+OKID model that identifies the mathematical models of R2R dynamic systems using measurements of the input (printing roller velocity) and output signals (register error) of the system. We further validate the performance of register error mitigation by applying MPC with the data-driven models. The overall DD-MPC approach has demonstrated its usefulness in register control for complex R2R systems when physical models are not available but reliable sensor data are accessible. The DD-MPC method can also achieve superior control performance in handling non-linear multi-input multi-output systems. For the future work, we will further explore other data-driven control methods and compare the performance of our methods with data-driven PID-type of controllers. We will test and mitigate the effects of variations in the form of disturbances in input data by modifying the system identification techniques and the DD-MPC controller accordingly. It is also important to further explore the effects of sensor noise in the output measurements and its effects on the identified system model.

ACKNOWLEDGEMENT

This material is based upon work supported by the National Science Foundation under Grant No.1907250 and Grant No.1943801. Any opinions, findings, and conclusions or recommendations expressed in this material are those of the authors and do not necessarily reflect the views of the National Science Foundation.

REFERENCES

[1] Seshadri, A., Pagilla, P. R., and Lynch, J. E., 2013. "Modeling print registration in roll-to-roll printing presses". *Journal of dynamic systems, measurement, and control,* ***135***(3), p. 031016.

[2] Chen, Z., He, J., Zheng, Y., Song, T., and Deng, Z., 2015.

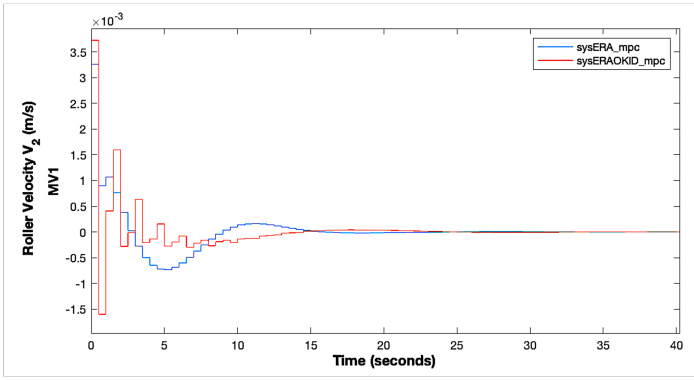

(a) CONTROL INPUT V_2

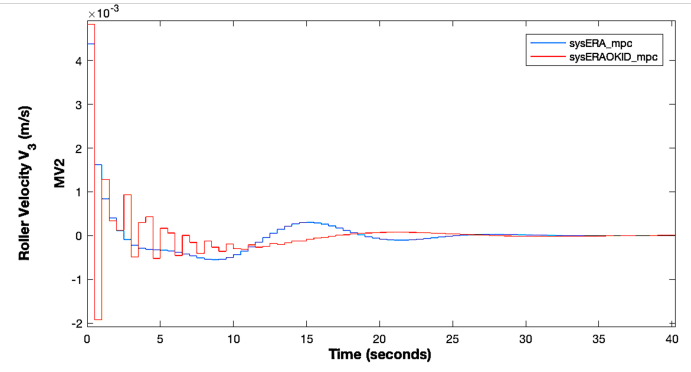

(b) CONTROL INPUT V_3

FIGURE 12: CONTROL INPUT RESPONSE TO INITIAL CONDITIONS WITH DD-MPC

"An optimized feedforward decoupling pd register control method of roll-to-roll web printing systems". *IEEE Transactions on Automation Science and Engineering,* ***13***(1), pp. 274–283.

[3] Yoshida, T., 2008. "Modeling and cooperative register control of gravure printing press". *Transactions of the Japan society of mechanical engineers C,* ***74***(738), pp. 339–345.

[4] Yan, J., and Du, X., 2020. "Web tension and speed control in roll-to-roll systems". In *Control Theory in Engineering*. IntechOpen, p. 209.

[5] Choi, K.-H., Tran, T. T., Ganeshthangaraj, P., Lee, K., Nguyen, M., Jo, J.-D., and Kim, D.-S., 2010. "Web register control algorithm for roll-to-roll system based printed electronics". In 2010 IEEE International Conference on Automation Science and Engineering, IEEE, pp. 867–872.

[6] Kang, H., and Lee, C., 2015. "Effect of tension on conductivity of gravure printed ag layer in roll-to-roll process". *International Journal of Precision Engineering and Manufacturing,* ***16***(1), pp. 99–104.

[7] Brandenburg, G., 1976. "New mathematical models for web tension and register error". In International IFAC Conference on Instrumentation and Automation in the Paper, Rubber and Plastics Industry, Brussels, Belgium, 1976, Vol. 1, p. 411.

[8] Pagilla, P. R., Siraskar, N. B., and Dwivedula, R. V., 2006. "Decentralized control of web processing lines". *IEEE Transactions on control systems technology,* ***15***(1), pp. 106–117.

[9] Kang, H., Lee, C., and Shin, K., 2013. "Modeling and compensation of the machine directional register in roll-to-roll printing". *Control Engineering Practice,* ***21***(5), pp. 645–654.

[10] Yoshida, T., Takagi, S., Muto, Y., and Shen, T., 2008. "Register control of sectional drive rotogravure printing press". In *Manufacturing systems and technologies for the new frontier*. Springer, pp. 417–420.

[11] Komatsu, H., Yoshida, T., Takagi, S., Shen, T., and Muto, Y., 2007. "Improvement of printing accuracy via web handling control in multi-colors printing machines". In 2007 International Conference on Control, Automation and Systems, IEEE, pp. 953–956.

[12] Kang, H., and Baumann, R. R., 2014. "Mathematical modeling and simulations for machine directional register in hybrid roll-to-roll printing systems". *International journal of precision engineering and manufacturing,* ***15***(10), pp. 2109–2116.

[13] Juang, J.-N., and Pappa, R. S., 1985. "An eigensystem realization algorithm for modal parameter identification and model reduction". *Journal of guidance, control, and dynamics,* ***8***(5), pp. 620–627.

[14] Juang, J.-N., Phan, M., Horta, L. G., and Longman, R. W., 1993. "Identification of observer/kalman filter markov parameters-theory and experiments". *Journal of Guidance, Control, and Dynamics,* ***16***(2), pp. 320–329.

[15] Pappa, R. S., Elliott, K. B., and Schenk, A., 1993. "Consistent-mode indicator for the eigensystem realization algorithm". *Journal of Guidance, Control, and Dynamics,* ***16***(5), pp. 852–858.

[16] Bath, P. E., Gaitonde, A., and Jones, D., 2022. "Reduced order aerodynamics and flight mechanics coupling for tiltrotor aircraft stability analysis". In AIAA SCITECH 2022 Forum, p. 0284.

[17] Brownell, M., Sinclair, A. J., and Singla, P., 2022. "A subspace method for shape estimation of flexible spacecraft membrane". In AIAA SCITECH 2022 Forum, p. 2378.

[18] Leshikar, C., and Valasek, J., 2022. "System identification flight testing of inverted v-tail small unmanned air system". In AIAA SCITECH 2022 Forum, p. 2408.

[19] Iyer, V. V., Johnson, E. N., and Singla, P., 2022. "Observer controller identification of a medium-weight co-axial octocopter". In AIAA SCITECH 2022 Forum, p. 1083.